de Haas–van Alphen Effect in Single Crystal MgB_2

E. A. Yelland and J. R. Cooper
Interdisciplinary Research Centre in Superconductivity and Department of Physics, University of Cambridge, Madingley Road, Cambridge CB3 0HE, United Kingdom

A. Carrington, N. E. Hussey, and P. J. Meeson
H. H. Wills Physics Laboratory, University of Bristol, Tyndall Avenue, BS8 1TL, United Kingdom

S. Lee, A. Yamamoto, and S. Tajima
Superconductivity Research Laboratory, International Superconducting Technology Center, Tokyo 135-0062, Japan
(Received 20 December 2001; published 10 May 2002)

We report observations of quantum oscillations in single crystals of the high temperature superconductor MgB_2. Three de Haas–van Alphen frequencies are clearly resolved. Comparison with band structure calculations strongly suggests that two of these come from a single warped Fermi surface tube along the c direction, and that the third arises from cylindrical sections of an in-plane honeycomb network. The measured values of the effective mass range from $(0.44-0.68)m_e$. By comparing these to calculated band masses, we find that the electron-phonon coupling strength λ is a factor of ~ 3 larger for the c-axis tube orbits than for the in-plane network orbit, in accord with recent microscopic calculations.

DOI: 10.1103/PhysRevLett.88.217002 PACS numbers: 74.25.Jb, 74.70.Ad

The discovery of high temperature superconductivity in MgB_2 [1] has led to great interest in this hexagonal layered compound. Early isotope effect work clearly showed that phonons are important [2], but subsequent experiments and calculations have revealed some unusual features, such as the possible existence of two distinct superconducting gaps [3–6], that may be associated with two different bands [7,8].

The band structure of MgB_2 has been calculated by several groups [9], and, recently, photoemission experiments [10] have confirmed its qualitative features. Studies of the de Haas–van Alphen (dHvA) effect provide crucial information about the electronic properties of metals. Observation of quantum oscillations allows the shape of the Fermi surface and the effective masses of carriers on individual Fermi sheets to be found. Then, together with band-structure calculations, electron-phonon coupling constants can be obtained [11].

In this Letter, we report a detailed study of the dHvA effect in single crystals of MgB_2. Three dHvA frequencies are clearly resolved in our data and can be assigned to two distinct, orthogonal Fermi surfaces parallel to the main symmetry axes of MgB_2 [9]. The effective masses corresponding to these three frequencies have been measured and compared with recent calculations. The comparison shows clearly that the electron-phonon enhancement is large for the c-axis tube and much smaller for the in-plane electronlike tube.

The single crystals used in this work were grown in Tokyo by high pressure synthesis, as described in Ref. [12]. Two crystals from the same batch were studied in parallel using sensitive piezoresistive cantilevers to measure the torque (Γ) [13,14]—crystal A at Cambridge using a ^{4}He cryostat with a 15 T magnet and crystal B at Bristol using a ^{3}He cryostat with an 18 T magnet. The dimensions of the crystals A and B were $230 \times 80 \times 20\ \mu m^3$ and $230 \times 200 \times 47\ \mu m^3$, respectively (the shortest side being along the c axis). Thermal contact between the crystals and nearby calibrated thermometers was ensured by immersion in ^{3}He or ^{4}He liquids or a few mbars pressure of exchange gas. Both cryostats had a single-axis low-temperature rotatable sample stage and angles were measured to a relative accuracy of at least 1°. For crystal A, the alignment was verified from the symmetry of high resolution, torque versus angle sweeps near the c axis at 15 T, while for B a correction of 6° was applied to make the dHvA frequencies symmetrical about the crystal axes. The data obtained in both sets of experiments were essentially identical.

Figures 1(a)–1(c) show torque versus magnetic field data [15] for both crystals as a function of angle, as the crystals were rotated from $B \parallel [001]$ ($\theta = 0°$) to [100] ($\theta = 90°$). The orientation of the c axis was determined from the platelet shape and the anisotropy of the upper critical field H_{c2}. As expected, the torque signal goes to zero at the principal symmetry directions ($\theta = 0°$ and 90°) but is already sizable only a few degrees away. The signal was easily resolved over a wide field range, giving well defined dHvA frequencies [see the fast Fourier transforms (FFTs) in Fig. 1(d)]. Two frequencies (F_1 and F_2) were observed for field sweeps carried out within $\sim 45°$ of the c axis [Fig. 1(a)], while only a single frequency F_3 was found for fields nearer the plane [Figs. 1(b) and 1(c)].

The dHvA signals were analyzed in the conventional way using the Lifshitz-Kosevich expression [11,16] for the

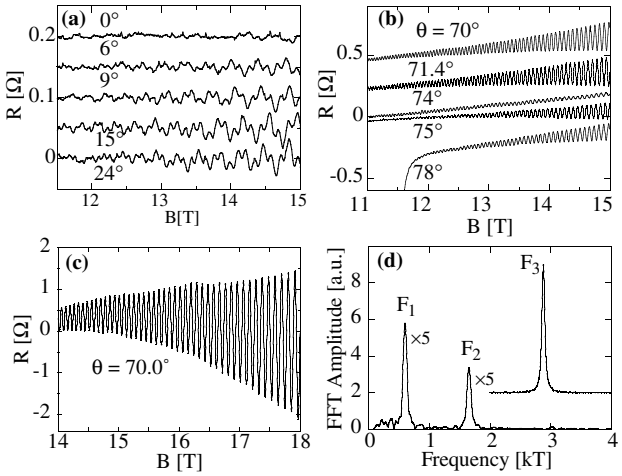

FIG. 1. (a)–(c) dHvA signals at several angles, rotating from [001] to [100]. (d) FFTs of the data at $\theta = 20°$ (F_1 and F_2) and 70° (F_3). The top and bottom panels show data for crystals A and B at 1.35 and 0.36 K, respectively.

oscillatory magnetization of a 3D Fermi liquid

$$M_{\rm osc} \propto B^{1/2} R_D R_T R_S \sin\left(\frac{2\pi F}{B} + \gamma\right), \qquad (1)$$

where F is the dHvA frequency [$F = (\hbar/2\pi e)A$, A is the extremal orbit area in $\mathbf{k}$ space]; γ is the phase; R_D, R_T, and R_S are the damping factors from impurity scattering, temperature (T), and spin splitting, respectively. $R_D = \exp(-\pi m_B/eB\tau)$, where m_B is the unenhanced or "bare" band mass [11,16] and τ is the scattering time. $R_T = X/(\sinh X)$ where $X = (\frac{2\pi^2 k_B m^*}{\hbar e})(\frac{T}{B})$, and m^* is the quasiparticle effective mass that is enhanced over m_B by both electron-electron and electron-phonon interactions, and m_e is the free-electron mass. The spin splitting phase factor is given by $R_S = \cos(n\pi g m_S/2m_e)$ where g is the Landé g factor for electrons in a given orbit, and m_S/m_B is the enhancement of the Pauli susceptibility from electron-electron interactions alone.

Figure 2 (upper panel) shows the angular dependence of the three dHvA frequencies observed in both crystals on rotating from $B \parallel [001]$ to [100]. There is excellent agreement between the two sets of data. The strong, nearly cosine angular dependence of F_1 and F_2 suggests that they arise from cylindrical sections along the c axis. Small deviations from a strict $1/\cos\theta$ dependence are shown in inset (a) of Fig. 2. Assuming a simple cosine c-axis dispersion [i.e., $\varepsilon_k = \hbar^2(k_x^2 + k_y^2)/2m - 2t_c\cos(ck_z)$], Yamaji [17] derived a formula which accounts for the "magic-angle" magnetoresistance maxima in quasi-2D organic superconductors. This gives the angular dependence of the two frequencies, $F_\pm$, arising from extremal areas of a single warped cylinder as

$$F_\pm(\theta)\cos\theta = (\hbar/2\pi e)[\pi k_f^2 \pm 4\pi m t_c J_0(ck_f \tan\theta)]. \qquad (2)$$

In this expression, the first term is the mean frequency $(\hbar/2\pi e)\pi k_f^2 = (F_1^0 + F_2^0)/2$, the prefactor of the second term $(\hbar/2\pi e)4\pi m t_c$ is $(F_2^0 - F_1^0)/2$, and J_0 is the Bessel function. Here F_1^0 and F_2^0 represent F_1 and F_2 at $\theta = 0$, and may be taken directly from the data, so this equation has no free parameters. The good agreement shown in inset (a) of Fig. 2 implies that F_1 and F_2 are the two extremal orbits of a single warped tube. As shown in inset (b) of Fig. 2, for the other orbit, $F_3\cos(90 - \theta)$ is remarkably constant (to within ±1% over ±40°), implying that it is cylindrical with very little warping.

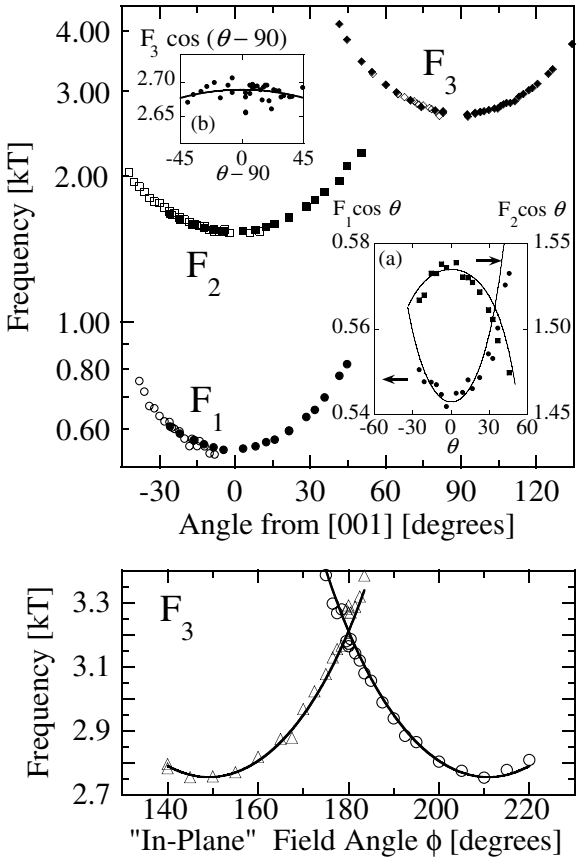

FIG. 2. Upper panel: Angular dependence of all three frequencies for a rotation between [001] and [100]. The open/closed symbols are data for crystals A/B, respectively. Inset (a) $F_1\cos\theta$ and $F_2\cos\theta$, with a fit to Eq. (2). Inset (b) $F_3\cos(\theta - 90)$. Lower panel: In-plane rotation plot for F_3, crystal A, with fits: $2685/(|\cos\beta\sin\phi| + |\sin\beta\cos 15\cos\phi|)$ where $\beta = 60$ or 120.

In Fig. 2 (lower panel), we show results obtained in a second experiment on crystal A in which the c axis was aligned at ~15° from the rotation axis and the magnetic field was rotated approximately within the basal plane. Two minima separated by 60° were observed, consistent with the hexagonal symmetry of MgB_2. The minimum value of F_3 in the upper panel agrees with that in the lower panel (after correcting for the 15° offset) showing that when $\theta = 90°$, in the upper panel, B lies along the [100] symmetry direction.

Temperature dependent studies were made for all three frequencies from 1.35 to 12 K (crystal A) and from 0.36 to 12 K (crystal B) and analyzed in the standard way by fitting the data to the damping factor R_T [Eq. (1)]. Fits for

crystal B are shown in Fig. 3, and values of m^* obtained in this way for both crystals are given in Table I. Measurements of m^* were made with B approximately 20° off a symmetry axis. The values in Table I have been multiplied by $\cos(\theta)$ [or $\sin(\theta)$] to correct for the usual angular dependence of the mass for a tubular band. This correction is less than 8%.

In the inset of Fig. 3 we show the angular dependence of the dHvA amplitude near [100], for both crystals. There is a pronounced dip between 14° and 18°. The slight difference for the two crystals is ascribed to small alignment errors about an axis perpendicular to the axis of rotation. No such dip was observed for F_1 and F_2. We believe the dip for F_3 is a "spin-zero," which is often observed in dHvA studies when the areas of spin-up and spin-down extremal orbits differ by a half-integral number of Landau quanta, leading to destructive interference in the oscillatory magnetization. This dip was shown to persist to at least 4.2 K. Since F_3 comes from a tubular surface, whose effective area $\propto 1/\cos\theta$, it is easily shown that the first zero occurs at an angle $\theta_{sz} = \cos^{-1}(g\frac{m_s}{m_e})$. As before, $\frac{m_S}{m_e}$ includes band effects and electron-electron enhancement but not electron-phonon enhancement of the standard type [11]. This is because the Pauli susceptibility of a metal can be enhanced by electron-electron interactions, e.g., by the Stoner mechanism, but not by the electron-phonon interaction. Our data give $\theta_{sz} = 18° \pm 3°$, and with $g = 2$ this gives $m_S = 0.476 \pm 0.007 m_e$.

The scattering rates of the three orbits were extracted using two procedures. We either subtracted a smoothly varying background and fitted the whole field sweep to Eq. (1)

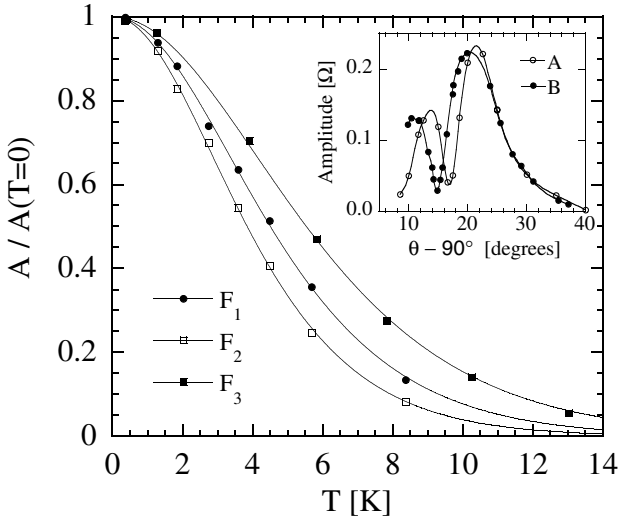

FIG. 3. Dependence of dHvA amplitude on temperature. The amplitude was measured by fitting the sine function [Eq. (1)] to 1.5 oscillations in the range 17.70 → 17.82 T for F_3 and 16.6 → 17.9 T for F_1 and F_2. The field was determined as the mean of $1/B$ in this window. The fit is to R_T in Eq. (1). Inset: Dependence of amplitude on angle for θ near [100] for crystals A (∘) and B (•). Raw data are shown for A at 15 T and 1.35 K [15] with data for B at 18 T and 0.36 K, normalized to the same peak height.

(or more precisely, $\Gamma \propto BM_{\rm osc}\,\partial \ln F/\partial\theta$) or fitted Eq. (1) to 1.5 oscillations in $1/B$ to give the dHvA amplitude with the thermal damping factor removed (A_s), as a function of B. In both cases we used the values of m^* from Table I in the R_T factor and set $R_S = 1$. In field regions where the sample is clearly in the normal state, the first method gives excellent fits to Eq. (1) for all three frequencies. Scattering times derived from fits for both crystals and all frequencies are shown in Table I. Making the approximation that all three frequencies arise from circular areas in **k** space, we can obtain k_F for each area and hence $v_F = \hbar k_F/m^*$, and the mean free path $\ell = v_F\tau$. These are also shown in Table I.

The second procedure removes thermal damping effects and reveals changes in the amplitude (A_s) versus $1/B$ plots caused by the onset of superconductivity below H_{c2}. As shown in Fig. 4 at angles of 70° or less, the usual exponential behavior is obtained [with slopes $\propto 1/\cos(90 - \theta)$ as expected for a tubular surface]. However, for angles nearer the plane, the Dingle plots become nonlinear because of additional damping caused by the growth of the superconducting gap, as has been observed in many superconductors (see, for example, Ref. [18]). This observation proves that our dHvA signals arise from MgB_2 rather than any impurity phase. The inset of Fig. 4 shows hysteresis arising from superconductivity that roughly corresponds to the onset of nonlinearity in the Dingle plot. However, the slope of the Dingle plot for $\theta = 81.7°$ remains high above 17 T, suggesting that the superconductivity has not been entirely suppressed in the reversible region.

Recently, detailed band structure calculations, including estimates of dHvA frequencies and masses, have been reported by three independent groups [19–21]. All calculations predict two warped cylinders along the c direction and two honeycomb networks in the basal plane. Comparison of the calculated frequencies with our experimental data shows that F_1 and F_2 arise from the smaller warped cylinder along the c axis while F_3 corresponds to the electronlike, in-plane tubular network whose median plane contains the A, H, and L symmetry points. The discrepancies with theory are less than 300 T (see Table I) which is only 0.2% of the area of the hexagonal Brillouin

TABLE I. Summary of results for both samples along with estimates of the frequencies and band masses from band-structure calculations (c) [20].

Orbit		F_1^0	F_2^0	F_3^0
Freq. [T]	A	535 ± 4	1530 ± 15	2688 ± 14
	B	546 ± 1	1533 ± 10	2685 ± 2
	c	728	1756	2889
Mass				
m^*/m_e	A	0.53 ± 0.01	0.680 ± 0.03	0.446 ± 0.01
	B	0.553 ± 0.01	0.648 ± 0.01	0.441 ± 0.01
m_B/m_e	c	0.251	0.312	0.315
τ [ps],	A	0.18 (500)	0.18 (660)	0.10 (750)
(ℓ [Å])	B	0.14 (380)	0.15 (580)	0.09 (680)

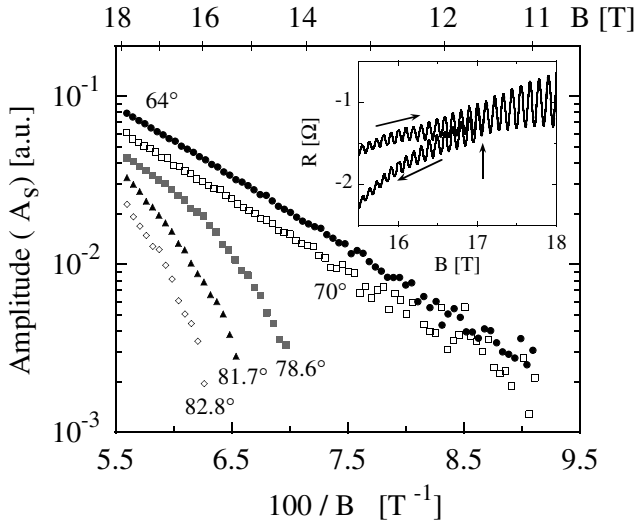

FIG. 4. dHvA amplitude (A_s) at 0.36 K versus inverse field for several values of θ. The inset shows up and down field sweeps at 81.7°. The field sweep direction is indicated. The vertical arrow marks the point where the hysteresis vanishes.

zone. Therefore, we can confidently compare our experimental values of m^* with the calculated values of m_B to obtain the electron-phonon enhancement factors (λ). We find $\lambda = (m^*/m_B - 1) = 1.20$, 1.08, and 0.40 for F_1, F_2, and F_3, respectively, which compare favorably with the calculated values $\lambda = 1.25$, 1.25, and 0.47 (Refs. [7,20,22]).

The detailed angular dependence of F_1, F_2, and F_3 has been calculated by Harima [19]. We find this also agrees with our data and supports the Yamaji analysis given above. The calculated values of m_B for F_3 also allow us to estimate the Stoner enhancement of the susceptibility. We find the enhancement $m_S/m_B - 1 = 0.51$ on this orbit, which is twice the calculated value of 0.26 [20].

The remaining discrepancy with theory concerns the absence of other dHvA orbits in the present study, particularly those arising from the second c-axis tube and the other in-plane network (band 4 in the notation of Ref. [19]). In view of the discrepancies of 300 T mentioned above, it is possible that the smallest orbits (<500 T) are actually even smaller or absent. The nonobservation of the other orbits could well be due to the relatively short mean-free-path of our crystals. Experiments to higher field and/or with purer crystals will clarify this point.

In summary, we have presented dHvA data for two single crystals of the new superconductor MgB_2 that are in excellent agreement with each other and in good agreement with the most recent band-structure calculations. The present work provides direct evidence that the electron-phonon interaction is large on the inner c-axis cylinder and much smaller on the in-plane honeycomb network. This supports microscopic theories of superconductivity that invoke two bands with very different properties [7,8].

J. R. C. is grateful to D. E. Farrell for introducing him to the cantilever technique during a sabbatical year in Cambridge in 1997 and to J. W. Loram and W. Y. Liang for their support. We thank S. Drechsler, H. Harima, S. M. Hayden, A. Janossy, J. Kortus, I. Mazin, M. Springford, G. Santi, and J. A. Wilson for helpful discussions. This work was supported by the NEDO (Japan) as Collaborative Research and Development of Fundamental Technologies for Superconductivity Applications and the EPSRC (U.K.). P. J. M. gratefully acknowledges the support of the Royal Society (London).

[1] J. Nagamatsu, N. Nakagawa, T. Muranaka, Y. Zenitani, and J. Akimitsu, Nature (London) **410**, 63 (2001).
[2] S. L. Bud'ko *et al.,* Phys. Rev. Lett. **86**, 1877 (2001).
[3] F. Bouquet *et al.,* Europhys. Lett. **56**, 856 (2001).
[4] X. K. Chen, M. J. Konstantinović, J. C. Irwin, D. D. Lawrie, and J. P. Franck, Phys. Rev. Lett. **87**, 157002 (2001).
[5] P. Szabó *et al.,* Phys. Rev. Lett. **87**, 137005 (2001).
[6] F. Manzano, A. Carrington, N. E. Hussey, S. Lee, A. Yamamoto, and S. Tajima, Phys. Rev. Lett. **88**, 047002 (2002).
[7] A. Y. Liu, I. I. Mazin, and J. Kortus, Phys. Rev. Lett. **87**, 087005 (2001).
[8] S. V. Shulga, S.-L. Drechsler, H. Eschrig, H. Rosner, and W. E. Pickett, cond-mat/0103154.
[9] See, for example, J. Kortus, I. I. Mazin, and K. D. Belashchenko, Phys. Rev. Lett. **86**, 4656 (2001).
[10] H. Uchiyama, K. M. Shen, S. Lee, A. Damascelli, D. H. Lu, D. L. Feng, Z.-X. Shen, and S. Tajima, cond-mat/0111152.
[11] D. Shoenberg, *Magnetic Oscillations in Metals* (Cambridge University Press, Cambridge, U.K., 1984).
[12] S. Lee, H. Mori, T. Masui, Y. Eltsev, A. Yamamoto, and S. Tajima, J. Phys. Soc. Jpn. **70**, 2255 (2001).
[13] C. Lupien, B. Ellman, P. Grütter, and L. Taillefer, Appl. Phys. Lett. **74**, 451 (1999).
[14] C. Bergemann, Ph.D. thesis, University of Cambridge, 1999.
[15] The conversion factor is $\simeq 10^{-10}$ N m/Ω (low field measurements in the diamagnetic state showed that this factor changed by less than ±5% between 1.4 and 10 K). Typical noise levels were $\pm 2 \times 10^{-13}$ N m.
[16] A. Wasserman and M. Springford, Adv. Phys. **45**, 471 (1996).
[17] K. Yamaji, J. Phys. Soc. Jpn. **58**, 1520 (1989).
[18] T. J. B. M. Janssen, C. Haworth, S. M. Hayden, P. J. Meeson, and M. Springford, Phys. Rev. B **57**, 11 698 (1998).
[19] H. Harima, cond-mat/0201452 [Physica (Amsterdam) C (to be published)]; (private communication).
[20] I. I. Mazin and J. Kortus, cond-mat/0201247.
[21] S. Elgazzar *et al.,* cond-mat/0201230; H. Rosner *et al.,* cond-mat/0203030.
[22] H. J. Choi, D. Roundy, H. Sun, M. L. Cohen, and S. G. Louie, cond-mat/0111182.